

1 **DNA sequence-selective C8-linked pyrrolbenzodiazepine(PBD)-heterocyclic polyamide**  
2 **conjugates show anti-tubercular specific activities**

3 Federico Brucoli,<sup>1\*</sup> Juan D. Guzman,<sup>2,†‡</sup> Mohammad A. Basher,<sup>4‡</sup> Dimitrios Evangelopoulos,<sup>2,3‡</sup>  
4 Eleanor McMahon,<sup>2</sup> Tulika Munshi,<sup>2‡</sup> Timothy D. McHugh,<sup>3</sup> Keith R. Fox,<sup>4</sup> and Sanjib Bhakta<sup>2</sup>

5 Author Affiliations

6 *<sup>1</sup>School of Science, Institute of Biomedical and Environmental Health Research (IBEHR), University of*  
7 *the West of Scotland, Paisley, PA1 2BE, Scotland, UK; <sup>2</sup>Department of Biological Sciences, Institute of*  
8 *Structural and Molecular Biology, Birkbeck College, University of London, London, WC1E 7HX, UK;*  
9 *<sup>3</sup>Centre for Clinical Microbiology, University College London, London, NW3 2PF, UK; <sup>4</sup>Centre for*  
10 *Biological Sciences, University of Southampton, Southampton SO17 1BJ, UK.*

11 \*Corresponding author. Tel: +44-(0)141-848-3264; E-mail: [federico.brucoli@uws.ac.uk](mailto:federico.brucoli@uws.ac.uk)

12 Present addresses:

13 †Departamento de Química y Biología, Universidad del Norte, Km 5 vía Puerto Colombia, Barranquilla  
14 081007, Colombia.

15 ‡The Francis Crick Institute, Mill Hill Laboratory, The Ridgeway, Mill Hill, London, NW7 1AA, UK.

16 ‡Institute of Infection and Immunity, St George's, University of London, Cranmer Terrace, London  
17 SW17 0RE, UK.

18 ‡These two authors equally contributed to this study.

19

20

21

## 22 **Abstract**

23 New chemotherapeutic agents with novel mechanisms of action are in urgent need to combat the  
24 tuberculosis pandemic. A library of twelve C8-linked pyrrolo[2,1-c][1,4]benzodiazepine(PBD)-  
25 heterocyclic polyamide conjugates (**1-12**) was evaluated for anti-tubercular activity and DNA sequence  
26 selectivity. The PBD-conjugates were screened against slow-growing *Mycobacterium bovis* BCG and  
27 *M. tuberculosis* H<sub>37</sub>Rv and fast-growing *Escherichia coli*, *Pseudomonas putida* and *Rhodococcus* sp.  
28 RHA1 bacteria. DNase I footprinting and DNA thermal denaturation experiments were used to  
29 determine the molecules' DNA recognition properties. The PBD-conjugates were highly selective for  
30 the mycobacterial strains and exhibited significant growth inhibitory activity against the pathogenic *M.*  
31 *tuberculosis* H<sub>37</sub>Rv, with compound **4** showing MIC values (MIC = 0.08 mg/L) similar to those of  
32 rifampin and isoniazid. DNase I footprinting results showed that the PBD-conjugates with three  
33 heterocyclic moieties had enhanced sequence selectivity and produced larger footprints with distinct  
34 cleavage patterns compared to the two-heterocyclic chain PBD-conjugates. DNA melting experiments  
35 indicated a covalent binding of the PBD-conjugates to two AT-rich DNA-duplexes containing either a  
36 central GGATCC or GTATAC sequence and showed that the polyamide chains affect the interactions  
37 of the molecules with DNA. The PBD-C8-conjugates tested in this study have a remarkable anti-  
38 mycobacterial activity and can be further developed as DNA-targeted anti-tubercular drugs.

## 39 **Keywords**

40 Drug discovery; DNA-minor groove binding agents; Pyrrolobenzodiazepines; Anti-tubercular agents;  
41 DNase I footprinting; *Mycobacterium tuberculosis*; HT-SPOTi

## 42 **1. Introduction**

43 Tuberculosis (TB) is a global health challenge, with 9 million new cases and 1.5 million deaths reported  
44 in 2013.<sup>1</sup> Furthermore, it is estimated that one third of the world's population is infected with  
45 *Mycobacterium tuberculosis*, accounting for a large reservoir of the bacilli.<sup>1</sup> The increasing incidence  
46 of TB is also linked to the steady increase in multi-drug and extensively-drug resistant tuberculosis  
47 (MDR/XDR-TB) strains, which renders TB difficult to treat.<sup>1,2</sup> Therefore, new antibiotics with novel

48 and pleiotropic modes of action are urgently needed to combat the TB pandemic, the rise of resistant  
49 bacilli and also provide new, safer and shorter drugs regimens. To this end, the complete reconstruction  
50 of the *M. tuberculosis* regulatory network <sup>3</sup> has laid the foundation for the development of DNA-  
51 targeted anti-mycobacterial agents. The ability of DNA sequence-selective agents to target specific  
52 promoter regions of the *M. tuberculosis* DNA can be exploited to disrupt the binding of mycobacterial  
53 transcription factors, induce bacterial cell death, overcome antimicrobial resistance and maximize  
54 therapeutic efficacy.

55 DNA-targeted chemotherapeutic agents are an important class of compounds, which have long attracted  
56 interest due to their distinctive mode of action involving specific interactions with predetermined DNA  
57 sequences.<sup>4-7</sup> Among these agents, pyrrolo[2,1-*c*][1,4]benzodiazepines (PBDs) have played a major  
58 role in cancer and antibacterial chemotherapy.<sup>8,9</sup> PBDs are a family of antitumour-antibiotics first  
59 isolated from cultures of *Streptomyces* species.<sup>10</sup> These molecules are DNA sequence-selective agents  
60 that covalently bind, via their N10-C11 imine functionality, to the C2-amino groups of guanine residues  
61 within the minor groove of DNA, spanning three DNA base pairs with a preference for Pu–G–Pu (where  
62 Pu = purine; G = guanine) sequences (**Figure 1**).<sup>9,11</sup> PBD monomers block transcription by inhibiting  
63 RNA polymerase activity in a sequence-specific manner.<sup>12</sup>

64 Since their discovery, several PBD analogues have been synthesised and extensively evaluated for their  
65 anticancer and antibacterial activities.<sup>8,13-17</sup> However, to our knowledge, there are only few studies  
66 focusing on the anti-mycobacterial activity of the PBDs. Taylor and Thurston reported that PBD  
67 dimers, in which two PBD units are tethered through a C8/C8'' diether linker to improve DNA-binding  
68 affinity and sequence specificity, exhibited notable activity against a panel of rapid and relatively rapid-  
69 growing mycobacteria, *Mycobacterium smegmatis*, *M. fortuitum*, *M. abscessus*, *M. phlei* and *M.*  
70 *aurum*.<sup>18</sup> Although showing anti-mycobacterial activity, the PBD dimers displayed significant  
71 cytotoxicity against human cell lines, especially compared to PBD monomers, and may be only used as  
72 “drug of last resort” to treat intractable infections caused by multi-drug resistant pathogens.<sup>19</sup> In another  
73 study, Kamal *et al.* showed that PBD-5,11-diones (PBD dilactams) inhibited the growth of

74 *Mycobacterium avium*, *M. intracellulare* and *M. tuberculosis*. PBD-dilactams stabilise duplex-DNA to  
75 a lesser extent than PBDs, as they lack the N10-C11 imine moiety responsible for the electrophilic  
76 alkylation of the C2-NH<sub>2</sub> of guanine bases, thus resulting in a non-covalent DNA interaction and  
77 reduced antibacterial and anticancer potency.<sup>9,20</sup>

78 In the present study, we investigated the anti-mycobacterial activity and DNA binding properties of a  
79 library of twelve C8-linked PBD-heterocyclic polyamide conjugates (**1-12**) (**Figure 2**), which were  
80 previously shown to have strong *in vitro* anticancer activities.<sup>21-23</sup> The di- or tri-heterocyclic polyamide  
81 chains of **1-12** are comprised of combinations of pyrrole (Py), imidazole (Im) and thiazole (Th) rings  
82 known for their ability to modulate the ligands' DNA-binding affinity.<sup>24</sup> C8-linked PBD-polyamide  
83 conjugates, unlike PBD dilactams, retain the ability to form covalent DNA-adducts, characteristic  
84 responsible for their improved cancer cell cytotoxicity and antibacterial activities,<sup>15</sup> and have a more  
85 favourable cytotoxicity profile compared to the PBD dimers.<sup>15,17</sup>

86 PBD-conjugates **1-12** were screened against slow-growing *Mycobacterium bovis* BCG and *M.*  
87 *tuberculosis* H<sub>37</sub>Rv and fast-growing *Escherichia coli*, *Pseudomonas putida* and *Rhodococcus sp.* and  
88 minimum inhibitory concentration values (MIC) were determined. Cytotoxicity against mouse  
89 macrophages RAW264.7 was also evaluated. The DNaseI footprinting experiments and thermal  
90 denaturation assays were used to evaluate the DNA recognition properties of **1-12**.

## 91 **2. Materials and methods**

### 92 *C8-linked PBD-heterocyclic polyamide conjugates*

93 The twelve PBD-conjugates **1-12** were synthesised and purified using published synthetic routes<sup>21, 22</sup>  
94 and dissolved in DMSO prior to use.

### 95 *Microorganisms and mammalian cells*

96 *Mycobacterium bovis* BCG Pasteur (ATCC 35734) and *M. tuberculosis* H<sub>37</sub>Rv (ATCC 27294), and  
97 *Escherichia coli* K12 (ATCC 53323), *Pseudomonas putida* KT2442 (ATCC 47054) and *Rhodococcus*

98 *sp.* RHA1 were used to screen the antibacterial activity of the PBD conjugates. Murine macrophages  
99 RAW264.7 (ATCC TIB71) were used in this study to evaluate the cytotoxicity of the PBD-conjugates.

100 *Mammalian macrophage cytotoxicity assay using resazurin assay*

101 The quantitation of eukaryotic cell toxicity was carried out as previously described.<sup>25</sup>

102 *Antibacterial assay against E. coli, P. putida and Rhodococcus sp.*

103 The evaluation of growth inhibition of the PDB-conjugates against *E. coli*, *P. putida* and *Rhodococcus*  
104 *sp.* was performed using the spot culture growth inhibition assay (SPOTi) in 24 well plates.<sup>26</sup> A seed  
105 culture of each bacteria was prepared in Luria Bertani (LB) broth and grown overnight at 37 °C with  
106 shaking at 200 rpm. *Rhodococcus sp.* was grown in LB broth at 30 °C with shaking at 200 rpm.  
107 Dilutions of the PBD-conjugates were performed in sterile DMSO at concentrations one thousand-fold  
108 more concentrated than the concentrations to be tested. 2 µL of each dilution were dispensed in each  
109 well of the 24 well plates, and 2 mL of LB agar were added to each well, and mixed. 2 µL of each  
110 inoculum containing approximately 10<sup>5</sup> colony-forming units (CFUs)/mL were carefully dispensed into  
111 the middle of the well on the surface of the solidified agar. The plate was incubated overnight at 37 °C  
112 for *E. coli* and *P. putida*, and at 30 °C for *Rhodococcus sp.* The plates were visually inspected and  
113 minimum inhibitory concentrations (MIC) values were recorded as the lowest concentration of PBD-  
114 conjugates where no growth was observed. Kanamycin was included as positive control.

115 *Anti-mycobacterial screening using HT-SPOTi*

116 *M. bovis* BCG and *M. tuberculosis* H<sub>37</sub>Rv were grown in Middlebrook 7H9 broth supplemented with  
117 0.02% (v/v) glycerol, 0.05% (v/v) tween-80 and 10% (v/v) albumin, dextrose and catalase (ADC; BD  
118 Biosciences) as a rolling culture at 2 rpm and 37 °C, and as a stand culture at 37 °C. The  
119 antimycobacterial activities of the compounds were tested following the HT-SPOTi guidelines.<sup>26,27</sup> HT-  
120 SPOTi is a high-throughput growth inhibition assay conducted in a semi-automated 96 well plate  
121 format. Compounds dissolved in DMSO at a final concentration of 50 mg/mL were serially diluted and

122 dispensed in a volume of 2  $\mu$ L into each well of a 96 well plate to which 200  $\mu$ L of Middlebrook 7H10  
123 agar medium kept at 55  $^{\circ}$ C supplemented with 0.05% (v/v) glycerol and 10% (v/v) OADC was added.  
124 Wells with no compounds (DMSO only) and isoniazid (positive control) were used as experimental  
125 controls. To all the plates, a drop (2  $\mu$ L) of mycobacterial culture containing  $2 \times 10^3$  CFUs was spotted  
126 in the middle of each well and the plates were incubated at 37  $^{\circ}$ C for 7 days. The MICs were determined  
127 as the lowest concentration of each compound where no mycobacterial growth was observed.

#### 128 *DNase I footprinting assay*

129 Footprinting reactions were performed as previously described<sup>28</sup> using the DNA fragments HexAfor  
130 and HexBRev, which together contain all 64 symmetrical hexanucleotide sequences. The DNA  
131 fragments were obtained by cutting the parent plasmids with *Hind*III and *Sac*I (*HexA*) or *Eco*RI and  
132 *Pst*I (*HexBRev*) and were labelled at the 3'-end with [ $\alpha$ -<sup>32</sup>P]dATP using reverse transcriptase. After  
133 gel purification the radiolabelled DNA was dissolved in 10 mM Tris-HCl pH 7.5 containing 0.1 mM  
134 EDTA, at a concentration of about 10 c.p.s per  $\mu$ L as determined on a hand held Geiger counter. 1.5  
135  $\mu$ L of radiolabelled DNA was mixed with 1.5  $\mu$ L ligand that had been freshly diluted in 10 mM Tris-  
136 HCl pH 7.5, containing 10 mM NaCl. The complexes were left to equilibrate for at least 12 hours  
137 before digesting with 2  $\mu$ L DNase I (final concentration about 0.01 units/ml). The reactions were  
138 stopped after 1 minute by adding 4  $\mu$ L of formamide containing 10 mM EDTA and bromophenol blue  
139 (0.1% w/v). The samples were then heated at 100  $^{\circ}$ C for 3 minutes before loading onto 8% denaturing  
140 polyacrylamide gels containing 8 M urea. Gels were fixed in 10% acetic acid, transferred to 3MM  
141 paper, dried and exposed to a phosphor screen overnight, before analysing with a typhoon  
142 phosphorimager.

#### 143 *DNA thermal denaturation studies*

144 Fluorescence melting curves were determined in a Roche LightCycler, using a total reaction volume of  
145 20  $\mu$ L. For each reaction the final oligonucleotide concentration was 0.25  $\mu$ M, diluted in 10 mM sodium  
146 phosphate pH 7.4 containing 100 mM NaCl. The experiments used the duplexes 5'-F-

147 AAAAGGATCCAAAA/5'-TTTTGGATCCTTTT-Q and 5'-F-AAAAGTATACAAAA/5'-  
148 TTTTGTATACTTTT-Q (F = fluorescein and Q = dabcyI). In a typical experiment the samples were  
149 first denatured by heating to 95 °C at a rate of 0.1 °C s<sup>-1</sup>. The samples were then maintained at 95 °C  
150 for 5 min before annealing by cooling to 25 °C at 0.1 °C s<sup>-1</sup> (this is the slowest heating and cooling rate  
151 for the LightCycler). They were held at 25 °C for a further 5 min and then melted by heating to 95 °C  
152 at 0.1 °C s<sup>-1</sup>. Recordings of the fluorescence emission at 520 nm were taken during both the melting  
153 steps as well as during annealing. The data were normalized to show the fractional change in  
154 fluorescence for each sample between the starting and final values. *T<sub>m</sub>* values were determined from  
155 the first derivatives of the melting profiles using the Roche LightCycler software.

### 156 3. Results

#### 157 *Growth inhibition of Mycobacterium spp.*

158 In **Table 1** are illustrated the results of the anti-tubercular and anti-bacterial screening, the cytotoxicity  
159 evaluation and the selectivity index (SI) of **1-12**. Compounds **1-12** were tested for growth inhibition  
160 against two slow-growing mycobacteria, *Mycobacterium bovis* BCG and *M. tuberculosis* H<sub>37</sub>Rv. The  
161 PBD-conjugates' MIC values against *M. tuberculosis* ranged from 0.08 to 5.19 mg/L, whereas the MIC  
162 values against *M. bovis* ranged from 0.04 to 20 mg/L. Dipyrrole-including PBD-conjugate **4** (Py-Py-  
163 PBD) exhibited the highest growth inhibitory activity against *M. tuberculosis* with a MIC value of 0.08  
164 mg/L. Compounds **5** (Py-Py-Im-PBD), **7** (Im-Im-Py-PBD), **9** (Py-Py-Th-PBD), **10** (Py-Th-Py-PBD)  
165 and **12** (Py-Py-Py-PBD) inhibited the growth of *M. tuberculosis* at 0.16 mg/L concentration. PBD-  
166 conjugate **1** (Py-Th-PBD) was active against *M. tuberculosis* and *M. bovis* at 0.31 and 0.16 mg/L,  
167 respectively, whereas compound **2** (Th-Py-PBD) inhibited the growth of both mycobacteria at 0.63  
168 mg/L. Compounds **6** (Py-Im-Py-PBD) and **8** (Im-Im-Im-PBD) were found to be 60-fold more active  
169 against *M. tuberculosis* (0.32 mg/L) than *M. bovis* BCG (20 mg/L), whereas PBD-conjugates **7, 9** and  
170 **10** were two-fold more active against *M. bovis* (0.08 mg/L) than *M. tuberculosis* (0.16 mg/L). Pyrrole-  
171 including PBD-conjugates **4** and **12** showed the highest growth inhibitory activity against *M. bovis* with  
172 a MIC of 0.04 mg/L. On the other hand, thiazole-including PBD-conjugates **3** (Th-Th-PBD) and **11**

173 (Th-Th-Th-PBD) exhibited the lowest growth inhibitory activity against both *M. tuberculosis* and *M.*  
174 *bovis* BCG with values of 5.19 and 20 mg/L, respectively. First-line anti-tubercular drugs isoniazid and  
175 rifampin were used as positive controls and inhibited the growth of both mycobacterial strains at 0.05  
176 mg/L.

177 *Antibacterial activity on E. coli* K12, *P. putida* KT2442 and *Rhodococcus sp.* RHA1

178 In order to evaluate the mycobacterial specificity of PBD-conjugates **1-12** in whole cell experiments  
179 and determine whether the compounds selectively affected slow-growing mycobacteria in comparison  
180 with fast-growing bacteria, we investigated the growth inhibitory activities of **1-12** against Gram-  
181 positive *Rhodococcus sp.* RHA1 and Gram-negative *Escherichia coli* K12 and *Pseudomonas putida*  
182 KT2442 bacteria. The results in **Table 1** show that the majority of PBD-conjugates (**1, 4-7, 9, 10** and  
183 **12**) had a significant growth inhibitory activity against *E. coli* and *Rhodococcus sp.* with a MIC value  
184 of 1.25 mg/L. Interestingly, PBD-conjugate **8** was 150-fold more active against *M. tuberculosis* (0.32  
185 mg/L) than Gram-negative *E. coli* and *P. putida* (>50 mg/L), whereas thiazole-containing PBD-  
186 conjugates **3** and **11** were 10-fold more active against *M. tuberculosis* (5.19 mg/L) than *E. coli*, *P. putida*  
187 and *Rhodococcus sp.* (>50 mg/L) strains. Tri-pyrrole-including PBD-conjugate **12** was active against  
188 *P. putida* at 5 mg/L, whereas compounds **4** and **5** inhibited the growth of this bacterium at 10 mg/L.  
189 Compounds **7, 9** and **10** were found to be approximately 300-fold more active against *M. tuberculosis*  
190 (0.16 mg/L) than *P. putida* (50 mg/L). The aminoglycoside antibiotic kanamycin was used as a positive  
191 control and inhibited the growth of *E. coli* and *P. putida* at 1.0 mg/L and *Rhodococcus sp.* at 10 mg/L.

192

193 *Macrophage RAW264.7 cytotoxicity*

194 The PBD-conjugates displayed various degrees of cytotoxicity against mammalian macrophages  
195 RAW264.7 with GIC<sub>50</sub> values ranging from 1.66 to 4.45 mg/L. The values of the Selectivity Index (SI),  
196 which is the ratio between macrophage half-growth inhibition concentration (GIC<sub>50</sub>) and MIC against  
197 the virulent H<sub>37</sub>Rv strain, ranged from 0.32 to 30.1, with PBD-conjugate **4** (Py-Py-PBD) exhibiting the



198 highest specificity (SI = 30.1) amongst the library members. PBD-conjugates **5**, **7**, **9**, **10** and **12**  
199 exhibited a SI of 10.4, whereas **1** had a SI of 14.4. Thiazole-including PBD-conjugates **3** and **11** showed  
200 the lowest specificity, with SI values of 0.46 and 0.32, respectively.

### 201 *DNase I footprinting*

202 DNase I footprinting was used to identify the binding sites of the PBD-conjugates, using the DNA  
203 fragments HexAfor and HexBrev,<sup>28</sup> which together contain all 64 possible symmetrical hexanucleotide  
204 sequences. The results are shown in **Figure 3**. The left hand panels show the footprints with 10  $\mu$ M of  
205 compounds **2**, **3**, **5**, **7**, **9** and **10** with HexAfor and HexBrev, while the two panels on the right show  
206 examples of the concentration dependence of the footprints with **5** and **9** on HexAfor. It is evident that  
207 compounds **5**, **9** and **10** produced large footprints in both HexAfor and HexBrev, while compound **7**  
208 produced fewer footprints including two shorter footprints (4a and b) within site 4. Each of these  
209 ligands produced a distinct cleavage pattern and the location of the major footprints is indicated in  
210 **Figure 4**. All these compounds contain three rings conjugated to the PBD. A few weaker footprints  
211 were seen with the compounds that only contain two conjugated rings. Compound **2**, which contains  
212 thiazole and pyrrole rings, produced footprints at sites 2, 4 and 8, while no footprints were seen with **3**,  
213 which contains two thiazole rings. It is clear that addition of the heterocycles affects the interaction of  
214 PBD with DNA. PBD-conjugates **5** (Py-Py-Im-PBD), **9** (Py-Py-Th-PBD) and **10** (Py-Th-Py-PBD)  
215 bound to sites 1, 2, 3 and 4 within HexBrev, and to sites 6, 7, 8 and 9 within HexAfor, while the footprint  
216 at site 5 in HexBrev is only evident with compounds **5** and **9**. Compound **7** bound to fewer sites with  
217 clear footprints limited to sites 3, 4a and 4b on HexBrev and site 8 on HexAfor. Although each ligand  
218 produced a characteristic cleavage pattern, it is noticeable that many of the footprints contained a short  
219 A/T tract followed by a guanine. The two right hand panels of **Figure 3** show the concentration  
220 dependence of the footprints with **5** and **9** on the HexAfor fragment. At 5  $\mu$ M concentration **5** produced  
221 a single footprint located in the lower part of site 8 within the sequence 5'-GCGCTTAAGTACT.  
222 Compound **9** produced footprints that persisted to lower concentrations, and the protections at the lower  
223 part of site 8 and in the centre of site 7 (5'-TAAACGTT) were still evident with 0.5  $\mu$ M ligand.

225 In order to further evaluate the contribution of the heterocyclic chains to the DNA recognition properties  
226 of the PBD-conjugates, the effects of the ligands on DNA-melting temperature were analysed using two  
227 fluorescently-labelled 14-mer DNA duplexes. These AT-rich DNA duplexes contained either a central  
228 GGATCC or GTATAC and the results with 0.5  $\mu\text{M}$  ligand are shown in **Figure 5**. It can be seen that  
229 all four of these ligands stabilised the duplexes and produced transitions at elevated temperatures. Since  
230 the ligands were covalently attached to the DNA, the  $T_m$  values of each transition did not change with  
231 the ligand concentration. However, the relative proportions of the different components were altered,  
232 so that a greater fraction of the higher  $T_m$  was evident with higher ligand concentrations. Each of these  
233 duplexes contains more than one guanine with which the conjugates could attach (two guanines for  
234 GTATAC and four for GGATCC) and further transitions were observed at higher ligand concentrations,  
235 as evident for **10** with both oligonucleotide duplexes. At a concentration of 0.5  $\mu\text{M}$  the ligand was in  
236 excess of the target duplex (0.25  $\mu\text{M}$ ). The fraction of the melting transition that has shifted to the  
237 higher temperature therefore indicates the proportion of the duplex that has been modified within the  
238 incubation period, though the absolute values of the melting transitions indicate the stabilization that is  
239 imparted by the bound ligand. The result of these experiments are summarised in **Table 2**. It can be  
240 seen that there is a good correlation between the large footprints produced by PBD-conjugates **9** and **10**  
241 with their greatest effect on the melting curves. At 0.5  $\mu\text{M}$  **9** shifted the entire melting curve to a higher  
242 temperature with both GTATAC ( $\Delta T_m = 29$ ) and GGATCC ( $\Delta T_m = 35$ ) with a small amount of  
243 uncomplexed duplex (5 and 10%, respectively). A similar effect is seen with **10** and GTATAC for  
244 which about 30% of the transition was shifted to an even higher temperature transition. In contrast, a  
245 significant amount of uncomplexed duplex (25%) was still evident with **10** and GGATCC, even though  
246 about 20% of the transition corresponded to a higher transition that suggested binding of a second  
247 ligand. The melting curves with 0.5  $\mu\text{M}$  **5** and **7** contained a large amount of the transition that  
248 corresponded to the uncomplexed duplex. **5** and **7** had a similar effect on GGATCC, though a greater  
249 fraction of GTATAC was bound by **7**.

#### 250 4. Discussion

251 The anti-mycobacterial evaluation of PBD-conjugates **1-12** revealed that these compounds have  
252 remarkable growth inhibitory activity against *M. tuberculosis* H<sub>37</sub>Rv. The nature and the length of the  
253 polyamide chain attached to the PBD unit had a significant influence on the molecules' anti-microbial  
254 activity and DNA-sequence selectivity. The presence of pyrrole rings in the polyamide chains affected  
255 the overall anti-tubercular activity of the compounds. The di-pyrrole-containing **4** had a MIC value of  
256 0.08 mg/L, which was comparable to those of isoniazid and rifampin, and an encouraging therapeutic  
257 window (SI = 30) that could be further improved in the second generation of PBD-based anti-  
258 tuberculosis agents. Although displaying some degrees of cytotoxicity towards mammalian cells, PBD-  
259 conjugate **4** represents a promising anti-TB therapeutic lead, particularly in light of the results generated  
260 by the large TB drug discovery campaign recently conducted by GlaxoSmithKline (GSK).<sup>29</sup>  
261 Researchers at GSK screened a 2 million proprietary-compounds collection for anti-mycobacterial  
262 activity against *M. tuberculosis* H<sub>37</sub>Rv and for cytotoxicity against mammalian cells (HepG2). A set  
263 of 177 bioactive-leads were identified displaying MIC <10 μM against H<sub>37</sub>Rv and selectivity  
264 (therapeutic) index (SI = HepG2IC<sub>50</sub>/MIC) ≥50. These values are of the same order of magnitude of  
265 those displayed by **4** (MIC = 0.13 μM and SI = 30), thus qualifying this compound as a promising lead  
266 that can be improved in subsequent medicinal chemistry work.

267 In addition, compounds **5, 7, 9, 10** and **12**, which exhibited the second best growth inhibitory activity  
268 of the series against the TB causing bacillus (MIC = 0.16 mg/L), all contained at least one pyrrole ring  
269 in their three-heterocyclic chains. PBD-conjugates with three-imidazole (**8**) and three-thiazole (**11**)  
270 chains showed a 2-fold and 30-fold decrease in *M. tuberculosis* growth inhibitory activity, respectively.  
271 This study also showed that the antimicrobial activity of PBD-conjugates **1-12** was highly selective  
272 against slow-growing mycobacteria *M. tuberculosis* and *M. bovis* compared to fast-growing bacteria *E.*  
273 *coli*, *P. putida* and *Rhodococcus sp.* The mechanism of action of the PBDs is unique and involves the  
274 covalent binding to guanine residues within the DNA minor-groove. The DNase I footprinting results  
275 showed that the PBD-conjugates bound with high affinity to large DNA sequences containing short A/T

276 stretches followed by a guanine residue, with **9** protecting the 5'-TAAACGTT sequence at a  
277 concentration as low as 0.5  $\mu$ M. This can be exploited to target discrete DNA sequences within the  
278 GC-rich mycobacterial genome and ultimately disrupt key enzymes and transcription factors. DNA  
279 melting studies revealed that thiazole-containing **9**, and to a lesser extent **10**, formed strong complexes  
280 and markedly shifted the melting curves of the two 14-mer DNA duplexes used in this study, thus  
281 confirming the significant DNA stabilisation properties of the compounds. In summary, these results  
282 show that **1-12** could serve as DNA-targeted therapeutic leads for the treatment of tuberculosis and  
283 further studies are underway to implement the potency and therapeutic index of these compounds.

## 284 **Acknowledgements**

285 We thank Professor Siamon Gordon for providing the RAW264.7 cell-line and Professor Simon Croft  
286 for granting access to the TB lab in the LSHTM. SB is a Cipla Distinguished Fellow in Pharmaceutical  
287 Sciences. Supported by MRC, UK (Grant Code: G0801956 to S.B.) to fund D.E. and T.M.'s post-  
288 doctoral studies at Birkbeck, University of London. J.D.G. received financial support from Colfuturo  
289 and a Bloomsbury Colleges studentship for his PhD studies. E.M. carried out a PhD rotation in S.B.'s  
290 lab funded by a Wellcome Trust Scholarship. M.A.B. is a Commonwealth Scholar in K.R.F.'s lab. The  
291 funders had no role in study design, data collection and analysis, decision to publish or preparation of  
292 the manuscript.

## 293 **References**

- 294 1. WHO. Global tuberculosis report 2012. Geneva: WHO. (2014)
- 295 2. Guzman JD, Gupta A, Bucar F, Gibbons S, Bhakta S. Antimycobacterials from natural sources:  
296 ancient times, antibiotic era and novel scaffolds. *Front Biosci.* 17:1861-1881 (2012)
- 297 3. Galagan JE, et al. The Mycobacterium tuberculosis regulatory network and hypoxia. *Nature.*  
298 499(7457):178-183 (2013)
- 299 4. Denny WA, Abraham DJ. Synthetic DNA-Targeted Chemotherapeutic Agents And Related  
300 Tumor-Activated Prodrugs. *In* Burger's Medicinal Chemistry and Drug Discovery. John Wiley  
301 & Sons, Inc., (2003)
- 302 5. Cozzi P, Mongelli N, Suarato A. Recent anticancer cytotoxic agents. *Current medicinal*  
303 *chemistry. Anti-cancer agents.* 4(2):93-121 (2004)
- 304 6. Hartley JA, Hochhauser D. Small molecule drugs - optimizing DNA damaging agent-based  
305 therapeutics. *Current opinion in pharmacology.* 12(4):398-402 (2012)
- 306 7. Baraldi PG, et al. DNA minor groove binders as potential antitumor and antimicrobial agents.  
307 *Med Res Rev.* 24(4):475-528 (2004)
- 308 8. Hartley JA. The development of pyrrolobenzodiazepines as antitumour agents. *Expert opinion*  
309 *on investigational drugs.* 20(6):733-744 (2011)

- 310 9. Antonow D, Thurston DE. Synthesis of DNA-interactive pyrrolo[2,1-c][1,4]benzodiazepines  
311 (PBDs). *Chemical reviews*. 111(4):2815-2864 (2011)
- 312 10. Leimgruber W, Stefanovic V, Schenker F, Karr A, Berger J. Isolation and characterization of  
313 anthramycin, a new antitumor antibiotic. *Journal of the American Chemical Society*.  
314 87(24):5791-5793 (1965)
- 315 11. Antonow D, et al. Solution structure of a 2:1 C2-(2-naphthyl) pyrrolo[2,1-  
316 c][1,4]benzodiazepine DNA adduct: molecular basis for unexpectedly high DNA helix  
317 stabilization. *Biochemistry*. 47(45):11818-11829 (2008)
- 318 12. Puvvada MS, et al. Inhibition of bacteriophage T7 RNA polymerase in vitro transcription by  
319 DNA-binding pyrrolo[2,1-c][1,4]benzodiazepines. *Biochemistry*. 36(9):2478-2484 (1997)
- 320 13. Hartley JA, et al. SG2285, a novel C2-aryl-substituted pyrrolobenzodiazepine dimer prodrug  
321 that cross-links DNA and exerts highly potent antitumor activity. *Cancer research*.  
322 70(17):6849-6858 (2010)
- 323 14. Hartley JA, Hamaguchi A, Suggitt M, Gregson SJ, Thurston DE, Howard PW. DNA interstrand  
324 cross-linking and in vivo antitumor activity of the extended pyrrolo[2,1-c][1,4]benzodiazepine  
325 dimer SG2057. *Investigational new drugs*. 30(3):950-958 (2012)
- 326 15. Rahman KM, et al. Antistaphylococcal activity of DNA-interactive pyrrolobenzodiazepine  
327 (PBD) dimers and PBD-biaryl conjugates. *Journal of Antimicrobial Chemotherapy*.  
328 67(7):1683-1696 (2012)
- 329 16. Rosado H, Rahman KM, Feuerbaum E-A, Hinds J, Thurston DE, Taylor PW. The minor  
330 groove-binding agent ELB-21 forms multiple interstrand and intrastrand covalent cross-links  
331 with duplex DNA and displays potent bactericidal activity against methicillin-resistant  
332 *Staphylococcus aureus*. *Journal of Antimicrobial Chemotherapy*. 66(5):985-996 (2011)
- 333 17. Rahman KM, et al. GC-Targeted C8-Linked Pyrrolobenzodiazepine–Biaryl Conjugates with  
334 Femtomolar in Vitro Cytotoxicity and in Vivo Antitumor Activity in Mouse Models. *J. Med.*  
335 *Chem*. 56(7):2911-2935 (2013)
- 336 18. Hadjivassileva T, Thurston DE, Taylor PW. Pyrrolobenzodiazepine dimers: novel sequence-  
337 selective, DNA-interactive, cross-linking agents with activity against Gram-positive bacteria.  
338 *Journal of Antimicrobial Chemotherapy*. 56(3):513-518 (2005)
- 339 19. Pepper CJ, Hambly RM, Fegan CD, Delavault P, Thurston DE. The novel sequence-specific  
340 DNA cross-linking agent SJG-136 (NSC 694501) has potent and selective in vitro cytotoxicity  
341 in human B-cell chronic lymphocytic leukemia cells with evidence of a p53-independent  
342 mechanism of cell kill. *Cancer research*. 64(18):6750-6755 (2004)
- 343 20. Antonow D, Jenkins TC, Howard PW, Thurston DE. Synthesis of a novel C2-aryl pyrrolo[2,1-  
344 c][1,4]benzodiazepine-5,11-dione library: effect of C2-aryl substitution on cytotoxicity and  
345 non-covalent DNA binding. *Bioorganic & medicinal chemistry*. 15(8):3041-3053 (2007)
- 346 21. Brucoli F, et al. An extended pyrrolobenzodiazepine-polyamide conjugate with selectivity for  
347 a DNA sequence containing the ICB2 transcription factor binding site. *J Med Chem*.  
348 56(16):6339-6351 (2013)
- 349 22. Brucoli F, et al. Novel C8-linked pyrrolobenzodiazepine (PBD)-heterocycle conjugates that  
350 recognize DNA sequences containing an inverted CCAAT box. *Bioorganic & medicinal*  
351 *chemistry letters*. 21(12):3780-3783 (2011)
- 352 23. Wells G, et al. Design, synthesis, and biophysical and biological evaluation of a series of  
353 pyrrolobenzodiazepine-poly(N-methylpyrrole) conjugates. *J Med Chem*. 49(18):5442-5461  
354 (2006)
- 355 24. Dervan PB. Molecular recognition of DNA by small molecules. *Bioorganic & medicinal*  
356 *chemistry*. 9(9):2215-2235 (2001)
- 357 25. Brucoli F, Guzman JD, Maitra A, James CH, Fox KR, Bhakta S. Synthesis, anti-mycobacterial  
358 activity and DNA sequence-selectivity of a library of biaryl-motifs containing polyamides.  
359 *Bioorganic & Medicinal Chemistry*. 23(13):3705-3711 (2015)
- 360 26. Guzman JD, et al. Antitubercular specific activity of ibuprofen and the other 2-arylpropanoic  
361 acids using the HT-SPOTi whole-cell phenotypic assay. *BMJ Open*. 3(6) (2013)
- 362 27. Danquah CA, Maitra A, Gibbons S, Faull J, Bhakta S. HT-SPOTi: A Rapid Drug Susceptibility  
363 Test (DST) to Evaluate Antibiotic Resistance Profiles and Novel Chemicals for Anti-Infective  
364 Drug Discovery. *Current protocols in microbiology*. 40:17 18 11-17 18 12 (2016)

- 365 28. Hampshire AJ, Fox KR. Preferred binding sites for the bifunctional intercalator TANDEM  
366 determined using DNA fragments that contain every symmetrical hexanucleotide sequence.  
367 *Analytical biochemistry*. 374(2):298-303 (2008)
- 368 29. Ballell L, et al. Fueling Open-Source Drug Discovery: 177 Small-Molecule Leads against  
369 Tuberculosis. *Chemmedchem*. 8(2):313-321 (2013)
- 370
- 371
- 372

373 **Figure Legends**

374

375 **Figure 1.** Schematic representation of the mechanism of action of PBDs involving the nucleophilic  
376 attack of the C2-NH<sub>2</sub> group of a guanine residue to the N10-C11 imine moiety of PBD within the DNA  
377 minor groove.

378

379 **Figure 2.** The library of twelve C8-linked PBD-heterocyclic polyamide conjugates **1-12** tested in this  
380 study.

381

382 **Figure 3.** DNase I footprinting patterns of the PBD-conjugates on the HexBrev and HexAfor DNA  
383 fragments. The first two panels show the results in the presence of 10 μM of each of the PBD-  
384 conjugates. The second two panels show the concentration dependence of footprints on HexAfor with  
385 **5** and **9**. Ligand concentrations (μM) are shown above each gel lane. The bars indicate the location of  
386 clear footprints. Tracks labelled GA are sequence markers specific for G and A, while con indicates  
387 DNase I cleavage in the absence of added ligand.

388

389 **Figure 4.** Sequences of HexAfor and HexBrev indicating the location of binding sites of the PBD-  
390 conjugates (underlined and numbered in sequences).

391

392 **Figure 5.** Fluorescence melting profiles for the DNA duplexes 5'-F-AAAAGGATCCAAAA/5'-  
393 TTTTGGATCCTTTT-Q and 5'-F-AAAAGTATACAAAA/5'-TTTTGTATACTTTT-Q (F =  
394 fluorescein and Q = dabcyI). The ligand concentration was 0.5 μM with 0.25 μM target duplex.

395

396

397

398

399

400

401

402

403

404

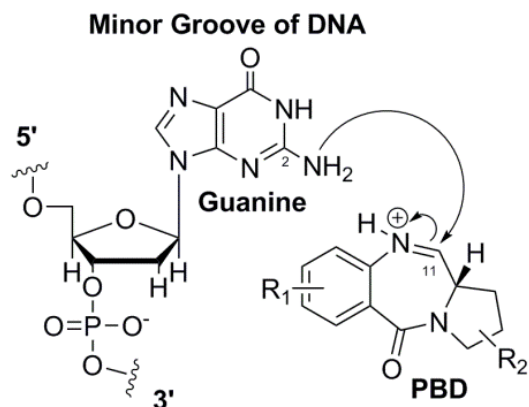
405

406 **Figures**

407

408

409 **Figure 1**



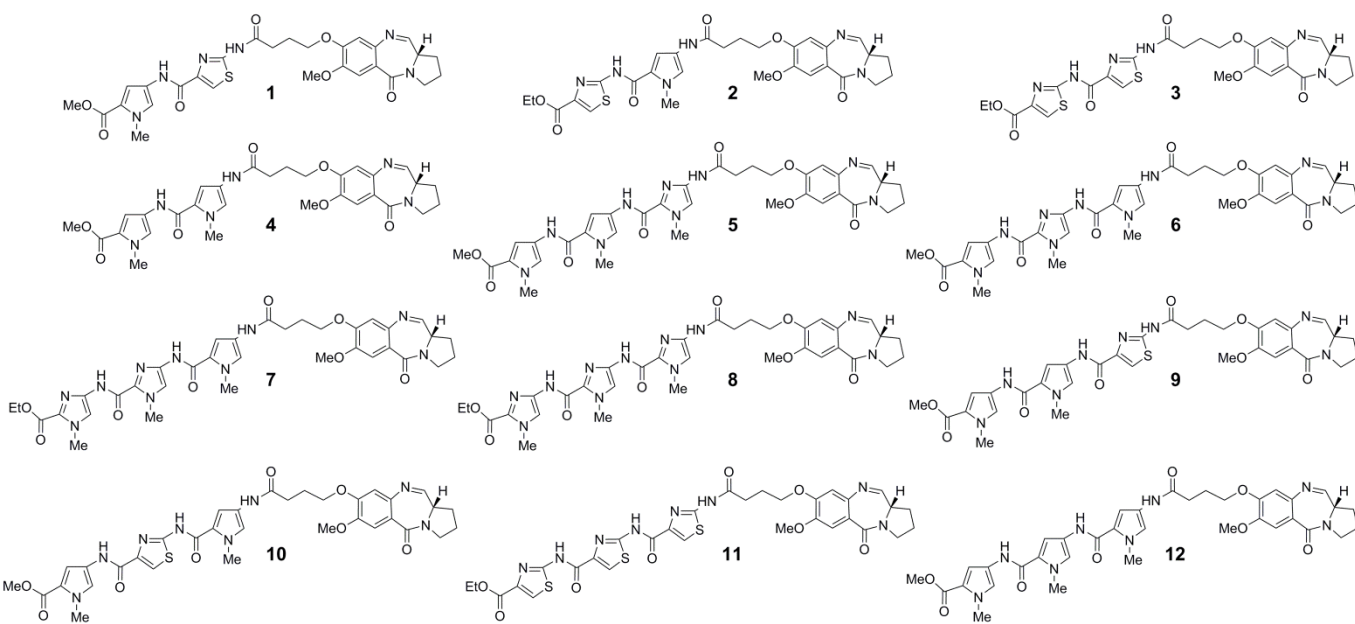
410

411

412

413

414 **Figure 2**



415

416

417

418

419

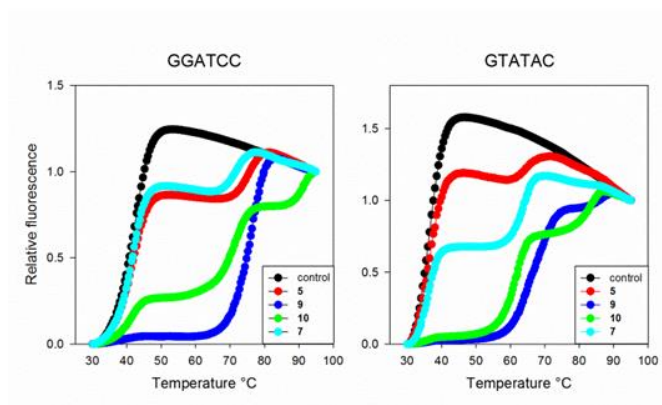
420

421





434 **Figure 5**



435

436

437

438

439

440

441

442

443

444

445

446

447

448

449

450

451

452

453

454

455

456

457

458

459

460

461

462 **Tables**

463

464 **Table 1.** Biological activity of PBD-conjugates 1-12.

Compound	MICs (mg/L)					GIC <sub>50</sub> RAW264.7 (mg/L)	SI <sup>a</sup>
	<i>Mycobacterium tuberculosis</i> H <sub>37</sub> Rv	<i>Mycobacterium bovis</i> BCG	<i>Escherichia coli</i> K12	<i>Pseudomonas putida</i> KT2442	<i>Rhodococcus sp.</i> RHA1		
<b>Py-Th-PBD (1)</b>	0.31	0.16	1.25	>20	1.25	4.45	14.4
<b>Th-Py-PBD (2)</b>	0.63	0.63	2.5	>50	5.0	2.41	3.83
<b>Th-Th-PBD (3)</b>	5.19	<20	>50	>50	>50	2.41	0.46
<b>Py-Py-PBD (4)</b>	0.08	0.04	1.25	10.0	1.25	2.41	30.1
<b>Py-Py-Im-PBD (5)</b>	0.16	0.16	1.25	10.0	1.25	1.66	10.4
<b>Py-Im-Py-PBD (6)</b>	0.32	<20	1.25	50.0	1.25	1.66	5.19
<b>Im-Im-Py-PBD (7)</b>	0.16	0.08	1.25	>50	1.25	1.66	10.4
<b>Im-Im-Im-PBD (8)</b>	0.32	<20	50.0	>50	10.0	1.66	5.19
<b>Py-Py-Th-PBD (9)</b>	0.16	0.08	1.25	50.0	1.25	1.66	10.4
<b>Py-Th-Py-PBD (10)</b>	0.16	0.08	1.25	>50	1.25	1.66	10.4
<b>Th-Th-Th-PBD (11)</b>	5.19	ND	>50	>50	>50	1.66	0.32
<b>Py-Py-Py-PBD (12)</b>	0.16	0.04	1.25	5.0	1.25	1.66	10.4
<b>Isoniazid</b>	0.05	0.05	ND	ND	ND	3000	60000
<b>Rifampin</b>	0.05	0.05	ND	ND	ND	700	14000
<b>Kanamycin</b>	ND	ND	1.0	1.0	10.0	ND	ND

465 <sup>a</sup>The SI was calculated by dividing the GIC<sub>50</sub> for RAW264.7 by the MIC against *M. tuberculosis* H<sub>37</sub>Rv

466

467

468

469 **Table 2.** Changes in melting temperature ( $\Delta T_m$ ) of the oligonucleotide duplexes in the presence of 0.5  $\mu$ M of each ligand and

470 the fraction of the transition that corresponds to the uncomplexed duplex.

	GGATCC $T_m = 41.7$ °C		GTATAC $T_m = 36.4$ °C	
	$\Delta T_m$	% free	$\Delta T_m$	% free
Py-Py-Im-PBD (5)	33	75	28	80
Im-Im-Py-PBD (7)	30	80	28	55
Py-Py-Th-PBD (9)	35	10	29	5
Py-Th-Py-PBD (10)	31	25	26	0

471

472

473

